RSC Advances

PAPER

Cite this: *RSC Adv.*, 2023, **13**, 24071

Cu(triNHC)-catalyzed polymerization of glycidol to produce ultralow-branched polyglycerol†

Kihyuk Sung,[a] Jinsu Baek,[b] Soonyoung Choi,[c] Byeong-Su Kim,[b] Sang-Ho Lee,[c] In-Hwan Lee *[d] and Hye-Young Jang *[a]

Received 3rd July 2023
Accepted 7th August 2023

DOI: 10.1039/d3ra04422j

rsc.li/rsc-advances

We have successfully synthesized a novel form of polyglycerol with an unprecedentedly low degree of branching (DB = 0.08–0.18), eliminating the need for glycidol protection. Leveraging the remarkable efficiency and selectivity of our Cu(triNHC) catalyst, comprising copper(I) ions and NHC ligands, we achieved a highly selective polymerization process. The proposed Cu-coordination mechanisms presented the formation of linear $L_{1,3}$ units while effectively suppressing dendritic units. Consequently, our pioneering approach yielded polyglycerol with an ultralow DB and exceptional yields. To comprehensively assess the physical properties and topology of the synthesized polyglycerol, we employed ^{1}H diffusion-ordered spectroscopy, size-exclusion chromatography, and matrix-assisted laser desorption/ionization-time of flight spectrometry. Remarkably, the ultralow-branched cyclic polyglycerol (DB = 0.08) synthesized at 0 °C showcased extraordinary characteristics, exhibiting the lowest diffusion coefficient and the highest molecular weight. This achievement establishes the significant potential of our polyglycerol with a low degree of branching, revolutionizing the field of biocompatible polymers.

Introduction

Polyglycerol is a highly regarded alternative to commercial poly(ethylene glycol) (PEG) due to its biocompatibility, water-solubility, low toxicity, and hydroxyl groups.[1–5] Compared to PEG, polyglycerol has a higher degree of water solubility and amorphous nature because of the hydroxy groups present in its polymer chain.[6] Furthermore, these hydroxy groups enable the polymer to bind to important biological molecules and metal ions for catalysis.[7–9] The tunable synthesis of polyglycerol has been widely investigated due to its versatile characteristics, including the control of its degree of branching (DB). By controlling the DB, the rheological and thermal properties of polyglycerol can be manipulated, which allows for a wide range of applications in the polymer industry.[4,10–12]

A number of techniques for the synthesis of polyglycerol with a high DB have been reported. For example, anionic,[13–15] cationic,[16–22] frustrated Lewis pair-catalyzed,[23] and heterogeneous double metal cyanide (DMC)-catalyzed polymerization[24] have been investigated for the synthesis of hyperbranched polyglycerol (*i.e.*, DB > 0.5). In contrast, the synthesis of low-branched polyglycerol has been more limited. To synthesize polyglycerol with an ultralow DB, protected glycidol ether has been utilized in anionic ring-opening polymerization, hydrolyzed diethylzinc catalysis, and tri-isobutyl aluminum/ammonium salts catalysis.[11,25] However, the deprotection of the alcohol is required after polymerization in these methods. The polymerization of unprotected glycidol with a low DB is challenging due to the facile chain growth at each hydroxy group in the polymer chain. Although various methods, such as kinetically controlled reactions with Sn(II) catalysts,[8] batch polymerization with DMC catalysts,[24] and aqueous epoxide ring-opening (AEROP),[26] have been employed to produce polyglycerol with a low DB (0.15–0.29), there is still a need for the development of a simple and efficient catalyst that can promote the synthesis of polyglycerol with an ultralow DB (Scheme 1).

In a recent report, we described the synthesis of Cu(triNHC) (triNHC = tri-*N*-heterocyclic carbene) complexes and their use as catalysts in click chemistry and CO_2 conversion.[27,28] In this study, it is suggested that both the Cu ions and the dissociated NHC ligands in the Cu(triNHC) complex could facilitate the polymerization of glycidol with high tunability. The Cu ions coordinate with the oxygen in the epoxide, and the NHC ligand induces the deprotonation of the glycidol hydroxyl group, which initiates polymerization. The resulting polymer is an ultralow-branched polyglycerol with cyclic topology, as illustrated in Scheme 1. Its physical properties were evaluated using several techniques, including matrix-assisted laser desorption/ionization-time of flight (MALDI-ToF) spectrometry, size-

[a]*Department of Energy Systems Research, Ajou University, Suwon 16499, Korea. E-mail: hyjang2@ajou.ac.kr; Tel: +82(031)-219-2555*

[b]*Department of Chemistry, Yonsei University, Seoul 03722, Korea*

[c]*Center for Advanced Specialty Chemicals, Korea Research Institute of Chemical Technology (KRICT), Ulsan 44412, Korea*

[d]*Department of Chemistry, Ajou University, Suwon 16499, Korea. E-mail: ilee@ajou.ac.kr*

† Electronic supplementary information (ESI) available. See DOI: https://doi.org/10.1039/d3ra04422j

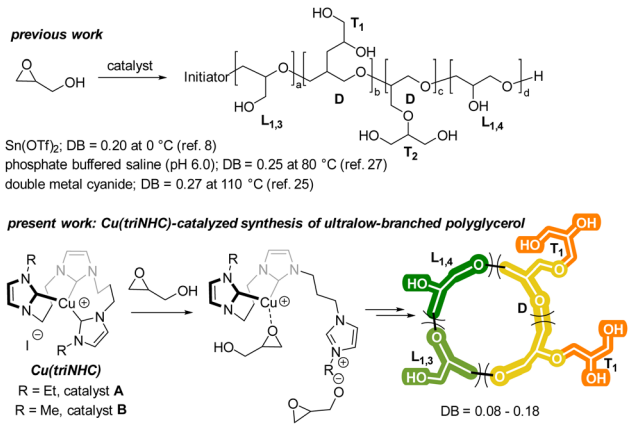

Scheme 1 Synthesis of polyglycerol with low DBs.

exclusion chromatography (SEC), differential scanning calorimetry (DSC), and ^{1}H diffusion-ordered spectroscopy (DOSY).

Experimental

General

Glycidol (96.0%), $Cu(OTf)_2$ (98.0%), 1,5,7-triazabicyclo[4.4.0]dec-5-ene (98%), copper iodide (99.999%) were obtained from Sigma Aldrich. 1,3-Bis(2,6-diisopropylphenyl)imidazole-2-ylidene (98.0%) was obtained from Tokyo Chemical Industry. Toluene (99.9%) was sourced from Samchun Chemicals. Glycidol and toluene were dried with CaH_2 and distilled prior to use. Proton nuclear magnetic resonance (^{1}H NMR) spectra were recorded with a Jeol Resonance ECZ600R (600 MHz) spectrometer. Chemical shifts are reported in delta (δ) units, parts per million (ppm) relative to the center of a peak at 2.50 ppm for DMSO-d_6. Coupling constants are reported in Hertz (Hz). Carbon-13 nuclear magnetic resonance (^{13}C NMR) spectra were recorded with a Jeol Resonance ECZ600R (150 MHz) spectrometer. Chemical shifts are reported in delta (δ) units, parts per million (ppm) relative to the center of a peak at 39.52 ppm for DMSO-d_6. ^{1}H diffusion-ordered spectroscopy (DOSY) was recorded on a Bruker AVANCE III HD 300 spectrometer at 25 °C. All samples were dissolved in DMSO-d_6. Matrix-assisted laser desorption/ionization time-of-flight (MALDI-ToF) measurement was performed using autoflex maX from Bruker. 2,5-Dihydroxybenzoic acid (DHB) was used as the matrix. For DMF–SEC, three polystyrene-gel columns [KD-802 (from Shodex); pore size, 150 Å; 8 mm i.d. × 300 mm, KD-803 (from Shodex); pore size, 500 Å; 8 mm i.d. × 300 mm, KD-804 (from Shodex); pore size, 1500 Å; 8 mm i.d. × 300 mm] were connected to a PU-4180 pump, a RI-4030 refractive-index detector, and a UV-4075 ultraviolet detector (JASCO); the flow rate was maintained at 1.0 ml min^{-1}. The columns were calibrated against 13 standard poly(ethylene glycol) (PEO) samples (Agilent Technologies; Mp = 980–811 500; M_w/M_n = 1.03–1.11) to analyze the obtained polymer samples. Differential scanning calorimetry (DSC) was conducted on polymer samples under a dry nitrogen flow (40 ml min^{-1}) in the temperature range of −70 to +70 °C at a heating or cooling rate of 10 °C min^{-1} on a Q2000 calorimeter (TA Instruments). Thermal gravimetric analysis (TGA) was conducted on the polymer sample under 20 ml min^{-1} of a dry nitrogen in the temperature range of +25 to +800 °C at a heating rate of 10 °C min^{-1} on STA 8122 High Temperature (Rigaku).

Experimental procedure for the polymerization of glycidol

Glycidol (148.2 mg, 2 mmol), catalysts (21.2 mg, 2 mol%), and toluene (1.0 ml) were added to the reaction vial. The mixture was stirred at the indicated temperature for 16 h under the nitrogen atmosphere. Then, the reaction mixture was washed with diethyl ether to remove the unreacted monomer. The product was dried at 50 °C for 1 day before obtaining the yield and sample analysis.

Experimental procedure for the catalyst recycling experiment

Glycidol (148.2 mg, 2 mmol), catalyst (21.2 mg, 2 mol%), and toluene (1.0 ml) were added to the reaction vial. The mixture was stirred at the indicated temperature for 16 h under the nitrogen atmosphere. After the reaction, glycidol (148.2 mg, 2 mmol) was added repeatedly in each cycle. Then, the reaction mixture was washed with diethyl ether to remove the unreacted monomer. The product was dried at 50 °C for 1 day before obtaining the yield and sample analysis.

Results and discussion

The polymerization of glycidol was conducted using catalyst **A** (2.0 mol%) in toluene at 25 °C, yielding a polymer with a 94% yield (entry 1 in Table 1). The DB of the resulting polymers was evaluated using the equation DB = $2D/(2D + L)$, where D is the fraction of dendritic units, and L is the fraction of linearly incorporated units (Table 1).[29] The relative abundance for each unit within the synthesized polymers is also shown in Fig. 1. Polymerization with catalyst **A** at 25 °C produced a polymer with a very low DB (0.18). When the polymerization was carried out at 0 °C with catalyst **A**, a longer reaction time was required, resulting in an 87% yield with a DB of 0.08 (entry 2 in Table 1), the lowest DB reported to date for polyglycerol synthesized using glycidol without a protection group (see ESI, Table S1†). The polymer synthesized at 0 °C contained more $L_{1,3}$ units and fewer D units than the polymer produced at 25 °C (Fig. 1). The higher number of $L_{1,3}$ units was associated with the low DB of the polymer.[30] The polymerization process with catalyst **A** was also investigated using different solvents (see ESI, Table S2†), and it was found that toluene produced the best results. Polyglycerol produced using this procedure exhibited insolubility in toluene, suppressing the growth of polymer chains with high molecular weight.

Catalyst **B**, which contains methyl-substituted NHC ligands, exhibited similar activity to catalyst **A** (entry 3 in Table 1). Using catalyst **B**, the relative abundance of D, $L_{1,3}$, $L_{1,4}$, and T_1 was 5.2%, 37%, 42%, and 16%, respectively (Fig. 1). Catalyst **B** produced more $L_{1,3}$ units and fewer D and T_1 units than catalyst **A**. Similar high yields and low DBs of polyglycerol were observed for both catalysts **A** and **B**, indicating that the influence of the terminal substituent of NHC ligands is negligible. Cu(triNHC)

Table 1 Polymerization of glycidol[a]

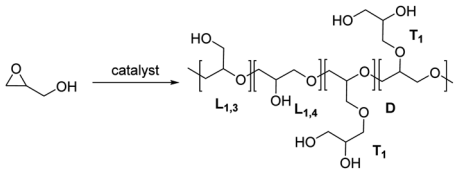

Entry	Catalyst	Temp (°C)	Time (h)	Yield (%)	DB	M_n (Da)	M_w/M_n	T_g (°C)	Diffusion coefficient ($m^2\ s^{-1}$)
1	**A**	25	16	94	0.18	2190	1.3	−13	0.93×10^{-10}
2	**A**	0	48	87	0.08	2660	1.6	−16	0.67×10^{-10}
3	**B**	25	16	85	0.12	2160	1.4	−18	0.92×10^{-10}
4	IPr	25	16	35	0.17	640	1.2	−34	1.25×10^{-10}
5	TBD	25	16	12	0.30	680	1.2	−23	1.31×10^{-10}
6	TBD	0	48	1.0	—	—	—	—	—
7	CuI	25	16	—	—	—	—	—	—
8	$Cu(OTf)_2$	25	16	98	0.41	1500	1.7	−20	—
9	$Cu(OTf)_2$	0	48	98	0.34	1100	1.3	−33	—

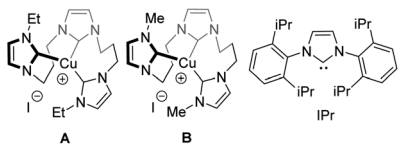

[a] Experimental conditions: the catalyst (2 mol%) and glycidol (2 mmol) in toluene (2.0 M) were stirred at the indicated temperature. DB was calculated by inverse-gated ^{13}C NMR using the equation "$2D/(2D + L)$" (D = dendritic unit; L = linear unit). M_n was measured by size-exclusion chromatography (SEC) calibrated with PEO standard in DMF (45 °C, flow rate 1.0 ml min^{-1}). Glass-transition temperature (T_g) was determined by differential scanning calorimetry (DSC) at a rate of 10 °C min^{-1}.

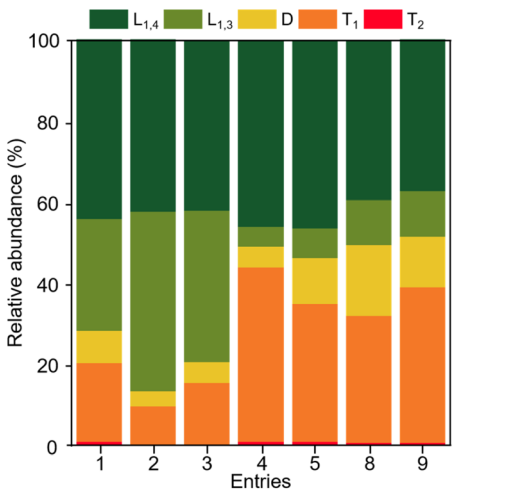

unit	entry 1	entry 2	entry 3	entry 4	entry 5	entry 8	entry 9
linear 1,4 ($L_{1,4}$)	44	42	42	46	46	39	37
linear 1,3 ($L_{1,3}$)	28	44	37	4.9	7.3	11	11
terminal T_1	20	9.7	16	43	34	31	39
terminal T_2	0.0	0.0	0.0	1.2	1.2	0.9	0.8
dendritic	8.0	3.8	5.2	5.1	12	18	12

Fig. 1 Relative abundance of the linear, terminal, and dendritic units for the polymers in Table 1 (calculated using inverse-gated ^{13}C NMR).

catalysts contain Cu ions and NHC ligands, where Cu ions induce the Cu-coordination mechanism, and the carbene ligand dissociated from Cu(triNHC) catalysts is basic enough to initiate deprotonation of glycidol. The function of the carbene ligand of Cu(triNHC) in the polymerization was evaluated as follows. The organic carbene compound, 1,3-bis(2,6-diisopropylphenyl)imidazole-2-ylidene (IPr) and the organic base, 1,5,7-triazabicyclo[4.4.0]dec-5-ene (TBD) were tested at room temperature, resulting in low polymer yields (entries 4 and 5 in Table 1).[31] The reaction using TBD at 0 °C produced a polymer with a yield of only 1.0% (entry 6 in Table 1). IPr produced polyglycerol with a relatively low DB but high relative abundance of terminal units (43% for T_1 and 1.2% for T_2 units), low molecular weight ($M_n = 640$), and low yield, indicating that IPr was not as effective as Cu(triNHC) catalysts (catalysts **A** and **B**) in promoting chain growth. In contrast, the reaction using TBD produced a polymer with a DB of 0.30, higher than that of catalyst **A** or **B** (entry 5 of Table 1). The Cu(I) catalyst without carbene ligands did not induce the desired polymerization (entry 7 in Table 1), while $Cu(OTf)_2$-catalyzed polymerization resulted in good yields at 25 °C and 0 °C (entries 8 and 9 of Table 1). $Cu(OTf)_2$-induced polymerization at 25 °C and 0 °C led to a DB of 0.41 and 0.34, respectively, with more D and T units observed than with the Cu(triNHC) catalyst. Overall, both Cu(I) ions and carbene ligands are essential for the low DB of polyglycerol and chain growth while maintaining high catalytic activity.

The topology of the polyglycerol was analyzed through MALDI-ToF analysis, as shown in Fig. 2. Polyglycerol obtained

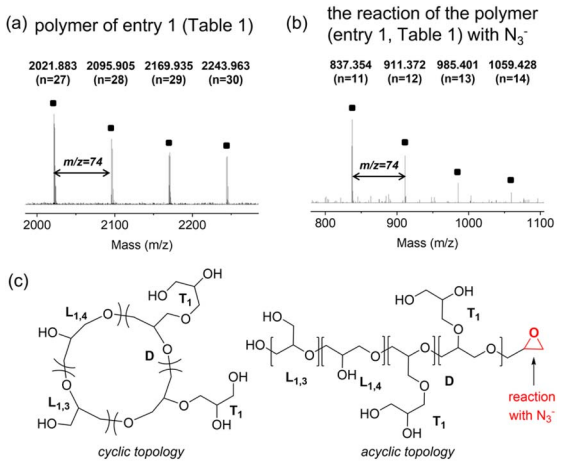

Fig. 2 (a) MALDI-ToF analysis of the polyglycerol produced using catalyst A (entry 1 in Table 1), (b) MALDI-ToF analysis of the polyglycerol after the reaction with N_3^-, and (c) cyclic and acyclic polyglycerol structures.

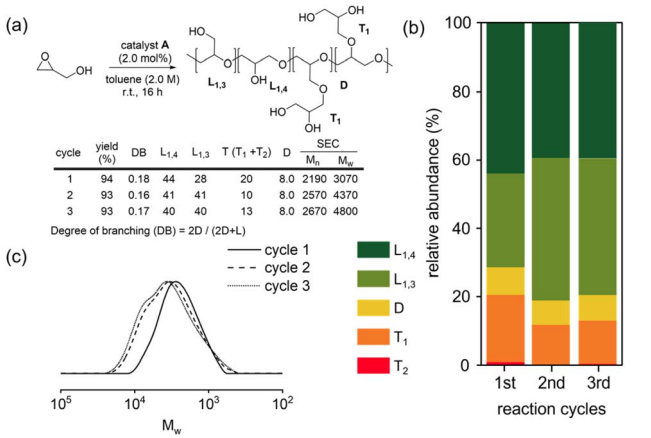

Fig. 3 (a) Recycling experiments, (b) the relative abundance of the linear, terminal, and dendritic units for each cycle calculated using inverse-gated ^{13}C NMR, and (c) SEC traces of the polyglycerols.

using catalyst **A** at 25 °C (entry 1 in Table 1) displayed signals that corresponded to $M_{observed}$ (Da) = $n \times 74.04 + Na^+$ with regularly spaced peaks of 74.04 Da, which represents the mass of glycidol (Fig. 2a). The signals could be attributed to cyclic polymers or acyclic polymers with an epoxy group at the chain end (Fig. 2c). To determine the polymer topology, polyglycerol (entry 1 in Table 1) was reacted with N_3^-. The addition of azide was not observed in the reaction mixture (Fig. 2b and S2†). The polymer synthesized at 0 °C with catalyst **A** showed major peaks that corresponded to $M_{observed}$ (Da) = $n \times 74.04 + Na^+$ (see ESI, Fig. S3†). On the other hand, the polyglycerol obtained using catalyst **B** at 25 °C displayed signals indicating the presence of cyclic polymers (see ESI, Fig. S4†). The polymers synthesized using IPr and TBD exhibited peaks of $M_{observed}$ (Da) = $n \times 74.04 + Na^+$, which were further confirmed to have cyclic topology through N_3^- addition reactions (see ESI, Fig. S5 and S6†). MALDI-ToF analysis of the polymer produced using $Cu(OTf)_2$ revealed the presence of both cyclic and acyclic structures (see ESI, Fig. S7 and S8†).

DOSY and SEC were employed to investigate the behavior of selected polyglycerol samples in solution. The diffusion coefficient obtained from DOSY provides information on the mobility of polymer molecules in fluid (Table 1 and Fig. S9–S15†), which is closely related to the hydrodynamic volume of the polymer. As the molecular weights obtained from SEC were closely related to the hydrodynamic volume, the correlation between the diffusion coefficient and the molecular weight (the hydrodynamic volume) of the polymers was examined. The polyglycerol samples for entries 1, 2, and 3 in Table 1 were analyzed using DMF–SEC, revealing an M_n of 2190, 2660, and 2160, respectively (see ESI, Fig. S16–S18†). The diffusion coefficients for these polymers were 0.93×10^{-10} m^2 s^{-1}, 0.67×10^{-10} m^2 s^{-1}, and 0.92×10^{-10} m^2 s^{-1}, respectively (Table 1). Entries 1 and 3 in Table 1 exhibited similar molecular weights and diffusion coefficients, while entry 2 had the lowest diffusion coefficient and the highest molecular weight. Previous research has shown that diffusion coefficients are influenced by several factors, including the DB, molecular weight, and topology of a polymer.[23] The low diffusion coefficient for the polymer listed as entry 2 in Table 1 resulted from its high molecular weight and low DB. Additionally, chain-end analysis using MALDI-ToF revealed that a small proportion of acyclic chains were present for this polymer (see ESI, Fig. S3a†). Thus, the effect of the topology of polyglycerol in explaining the low diffusion coefficient cannot be completely ruled out. The polyglycerol listed as entry 4 in Table 1, which had a low molecular weight according to SEC analysis (M_n = 637), had a higher diffusion coefficient (1.25×10^{-10} m^2 s^{-1}) than entry 1 (M_n = 2190 and diffusion coefficient = 0.93×10^{-10} m^2 s^{-1}), though they exhibited similar DBs (0.18 for entry 1 and 0.17 for entry 4) and the same cyclic topology. Therefore, this comparison confirmed the close correlation between the molecular weight and the diffusion coefficient.[32] Overall, there is a correlation that can be established between the diffusion coefficient, molecular weight, and hydrodynamic volume of polymers that have similar DB and topology. The glass transition temperature (T_g) of the polyglycerols was also measured (Table 1 and Fig. S33†). The T_g of polyglycerols can be affected by the intra- and intermolecular hydrogen bonding of the polymer chains arising from the DB, molecular weight, and topology. A comparison of T_g values for entries 1 and 4 showed that T_g was correlated with the molecular weights when the DBs were similar. The thermal property of polyglycerol was assessed using thermal gravimetric analysis (TGA), which revealed decomposition occurring at 393 °C (Fig. S34†).

The Cu(triNHC) catalyst exhibited a significant polyglycerol yield with remarkably low branching. The coordination of the three NHC ligands enhances the stability of Cu(I) catalysts, effectively preventing oxidation to Cu(II). Accordingly, we conducted accumulation experiments by adding glycidol to the reaction mixture to assess the recyclability of catalyst **A** (Fig. 3a). The yields for the second and third cycles remained high. The analysis of the unit distribution was conducted using the

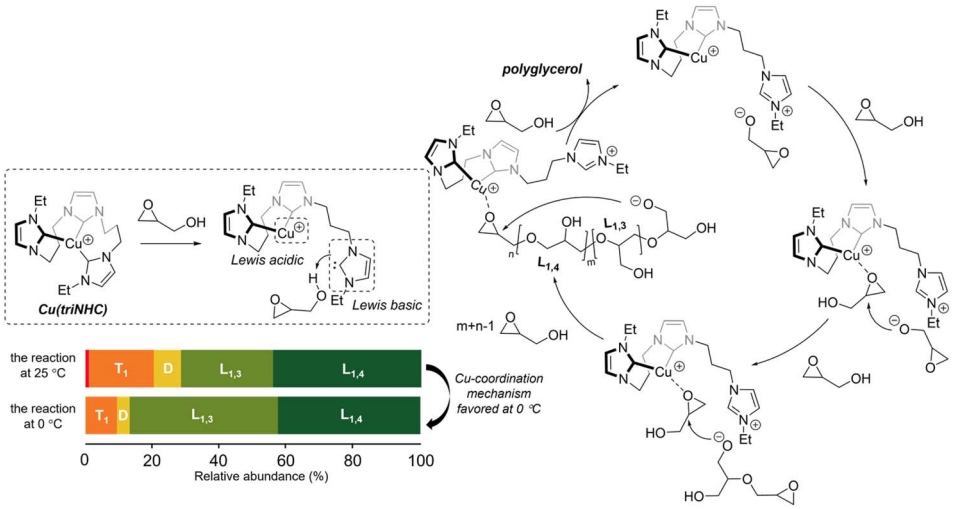

Scheme 2 Cu-coordinated mechanisms for polyglycerol synthesis.

reaction mixture (Fig. 3b). Interestingly, the proportion of $L_{1,3}$ units increased and that of T units decreased in the second and third cycles. Additionally, the SEC traces displayed a shift toward a higher molecular weight region and exhibited a bimodal distribution with an increase in the number of accumulation cycles (Fig. 3c). This finding indicates that the initiation process from the freshly added glycidol monomer may compete with the chain-extension process from the alcohol end-group of the pre-existing polyglycerol during the accumulation cycles. However, because polyglycerol is insoluble, additional glycidols were reacted with Cu(triNHC) catalysts to induce new chain growth from glycidol. The polymer chain growth from the pre-existing polyglycerol was not as facile as the formation of new chains from glycidol.

Polyglycerol synthesis can occur *via* several mechanisms, including the activated chain end (ACE), activated monomer (AM), and metal-coordination mechanisms.[16,19,24,26] In the case of the Cu(triNHC)-catalyzed reaction, the reaction mechanism was investigated based on the catalyst structure and the polymer chain units (Scheme 2). In our previous studies, it was found that Cu(triNHC) dissociates a carbene ligand to deprotonate the alcohol for the reaction.[28] Similarly, in this study, the reaction begins with the deprotonation of glycidol by the dissociated carbene ligand from the Cu catalyst. The proposed Cu complex having a protonated imidazolium group was observed by ^{1}H NMR of the reaction mixture (Fig. S35†). The catalytic reaction in dioxane which did not exhibit the polymer formation showed no dissociation of carbene ligand in the reaction mixture (Fig. S35†). When the glycidol alkoxide, located proximal to the imidazolium ion, adds to Cu-coordinated glycidol without proton exchange of resulting alkoxides, it leads to the production of $L_{1,3}$ units.[24] The Cu complex coordinated with the epoxide intermediate was observed by ESI-MS (see the ESI, Fig. S36†). On the other hand, the addition of glycerol alkoxide to the epoxide, followed by proton exchange forming terminal alkoxides, results in the formation of $L_{1,4}$ units. Finally, the Cu(triNHC)-catalyzed intramolecular reaction of the epoxide and the alkoxide at each end of the polymer chain produces a cyclic polymer. The Cu-coordination mechanism suppressing proton exchange is more strongly favored at 0 °C than at 25 °C, resulting in more $L_{1,3}$ units and a lower DB than the reaction at room temperature. Because this reaction is initiated by catalysts without additional anionic initiators, and the proton exchange is limited compared to anionic polymerization, the formation of dendritic units is suppressed, resulting in lower DB values. Poor polymerization results with the use of TBD at 0 °C suggest that base-induced anionic polymerization is likely to be suppressed at low temperatures. Overall, the superior activity of the Cu(triNHC) catalyst in producing polyglycerol with an ultralow DB and a cyclic topology was the result of the Cu-coordinated reaction of glycidol and glycidol alkoxide at the proximal carbenes inside the catalyst reaction sphere.[24,33,34]

Conclusions

We demonstrated the synthesis of polyglycerol with a low degree of branching and a cyclic topology using Cu(triNHC) catalysis. The unique structure of Cu(triNHC), which contains Cu ions and NHC ligands, facilitated the polymerization of glycidol with an extremely low DB. Glycidol alkoxides generated by the NHC ligand were provided to the Cu-coordinated glycidol, which promoted efficient polymerization with suppressed proton transfer and favored the formation of $L_{1,3}$ units. Consequently, the higher number of $L_{1,3}$ units and the lower number of $L_{1,4}$ and D units resulted in polyglycerol with an ultralow DB. The high stability of the Cu(triNHC) catalyst was demonstrated in a recycling experiment, with high catalytic activity observed up to a third cycle. The obtained polyglycerol's topology, diffusion coefficient, molecular weight, and T_g were analyzed using MALDI-ToF, DOSY, SEC, and DSC. In comparison to previous research that primarily focused on synthesizing highly branched polyglycerols, the development of practical methods to produce cyclic ultralow-branched polyglycerols without glycidol protection is relatively rare. Therefore, our

findings of Cu(triNHC)-catalyzed protocols expand the possibilities for using polyglycerol in the polymer and biomaterial industries.

Author contributions

H.-Y. Jang: conceptualization, supervision, writing original draft, and review & editing. K. Sung: investigation and formal analysis. J. Baek, S. Choi: formal analysis. B.-S. Kim, S.-H. Lee, I.-H. Lee: review & editing.

Conflicts of interest

There are no conflicts to declare.

Acknowledgements

This study was supported by the Carbon to X Program (No. 2020M3H7A1098283) and National Research Foundation Program (No. 2022R1A2C1004387) by the Ministry of Science and ICT, and Basic Science Research Program (No. 2021R1A6A1A10044950) by the Ministry of Education, Republic of Korea.

Notes and references

1 R. K. Kainthan, J. Janzen, E. Levin, D. V. Devine and D. E. Brooks, *Biomacromolecules*, 2006, **7**, 703–709.
2 C. Siegers, M. Biesalski and R. Haag, *Chem.–Eur. J.*, 2004, **10**, 2831–2838.
3 Solvay Chemicals, *Polyglycerols in Industrial Applications*, 2005, **http://www.solvaychemicals.com/**.
4 M. Schömer, C. Schüll and H. Frey, *J. Polym. Sci., Part A: Polym. Chem.*, 2013, **51**, 995–1019.
5 S. Abbina, S. Vappala, P. Kumar, E. M. J. Siren, C. C. La, U. Abbasi, D. E. Brooks and J. N. Kizhakkedathu, *J. Mater. Chem. B*, 2017, **5**, 9249–9277.
6 M. Schömer and H. Frey, *Macromolecules*, 2012, **45**, 3039–3046.
7 M. Calderón, M. A. Quadir, S. K. Sharma and R. Haag, *Adv. Mater.*, 2010, **12**, 190–218.
8 B. R. Spears, J. Waksal, C. McQuade, L. Lanier and E. Harth, *Chem. Commun.*, 2013, **49**, 2394–2396.
9 K. R. Kumar, K. N. Kizhakkedathu and D. Brooks, *Macromol. Chem. Phys.*, 2004, **205**, 567–573.
10 D. Wilms, S.-E. Stiriba and H. Frey, *Acc. Chem. Res.*, 2010, **43**, 129–141.
11 A. Thomas, S. S. Müller and H. Frey, *Biomacromolecules*, 2014, **15**, 1935–1954.
12 S. Y. Lee, M. Kim, T. K. Won, S. H. Back, Y. Hong, B.-S. Kim and D. J. Ahn, *Nat. Commun.*, 2022, **13**, 34300.
13 A. Sunder, R. Hanselmann, H. Frey and R. Mülhaupt, *Macromolecules*, 1999, **32**, 4240–4246.
14 R. K. Kainthan, E. B. Muliawan, S. G. Hatzikiriakos and D. E. Brooks, *Macromolecules*, 2006, **39**, 7708–7717.
15 C. Schubert, M. Schömer, M. Steube, S. Decker, C. Friedrich and H. Frey, *Macromol. Chem. Phys.*, 2018, **219**, 1700376.
16 R. Tokar, P. Kubisa, S. Penczek and A. Dworak, *Macromolecules*, 1994, **27**, 320–322.
17 A. T. Royappa, M. L. Vogt and V. Sharma, *J. Appl. Polym. Sci.*, 2004, **91**, 1344–1351.
18 I. Asenjo-Sanz, A. Veloso, J. I. Miranda, J. A. Pomposo and F. Barroso-Bujans, *Polym. Chem.*, 2014, **5**, 6905–6908.
19 E. Mohammadifar, A. Bodaghi, A. Dadkjajtehrani, A. N. Kharat, M. Adeli and R. Haag, *ACS Macro Lett.*, 2017, **6**, 35–40.
20 M. Dadkhah, H. Shamlooei, E. Mohammadifar and M. Adeli, *RSC Adv.*, 2018, **8**, 217–221.
21 S. E. Kim, H. J. Yang, S. Choi, E. Hwang, M. Kim, H.-J. Paik, J.-E. Jeong, Y. I. Park, J. C. Kim, B.-S. Kim and S.-H. Lee, *Green Chem.*, 2022, **24**, 251–258.
22 M. A. A. Assiri, E. G. Urreizti, C. A. Pagnacco, E. Gónzalez de San Román and F. Barroso-Bujans, *Eur. Polym. J.*, 2022, **171**, 111194.
23 S. E. Kim, Y.-R. Lee, M. Kim, E. Seo, H.-J. Paik, J. C. Kim, J.-E. Jeong, Y. I. Park, B.-S. Kim and S.-H. Lee, *Polym. Chem.*, 2022, **13**, 1243–1252.
24 C. H. Tran, M. W. Lee, S. A. Kim, H. B. Jang and I. Kim, *Macromolecules*, 2020, **53**, 2051–2060.
25 A. Haouet, M. Sepulchre and N. Spassky, *Eur. Polym. J.*, 1983, **19**, 1089–1098.
26 B. R. Spears, M. A. Marin, J. Montenegro-Burke, B. C. Evans, J. McLean and E. Harth, *Macromolecules*, 2016, **49**, 2022–2027.
27 C. Seo, Y.-J. Cheong, W. Yoon, J. Kim, J. Shin, H. Yun, S.-J. Kim and H.-Y. Jang, *Organometallics*, 2021, **40**, 16–22.
28 C. Seo, S. E. Kim, H. Kim and H.-Y. Jang, *ACS Sustainable Chem. Eng.*, 2022, **10**, 5643–5650.
29 D. Hölter, A. Burgath and H. Frey, *Acta Polym.*, 1997, **48**, 30–35.
30 C. Schubert, M. Schömer, M. Steube, S. Decker, C. Friedrich and H. Frey, *Macromol. Chem. Phys.*, 2018, **219**, 1700376.
31 N. E. Kamber, W. Jeong, S. Gonzalez, J. L. Hedrick and R. M. Waymouth, *Macromolecules*, 2009, **42**, 1634–1639.
32 W. Li, H. Chung, C. Daeffler, J. A. Johnson and R. H. Grubbs, *Macromolecules*, 2012, **45**, 9595–9603.
33 Y.-J. Huang, X.-H. Zhang, Z.-J. Hua, S.-L. Chen and G.-R. Qi, *Macromol. Chem. Phys.*, 2010, **211**, 1229–1237.
34 J. Ai, X. Min, C.-Y. Gao, H.-R. Tian, S. Dang and Z.-M. Sun, *Dalton Trans.*, 2017, **46**, 6756–6761.